

## IMPROVEMENT OF PHOTOVOLTAIC PERFORMANCE OF DYE SENSITIZED SOLAR CELLS BY PRE-DYE TREATING OF ZNO NANOPARTICLES

*Rajat Biswas, Joy Sarkar, Suman Chatterjee*

Department of Physics, University of North Bengal, Raja Rammohunpur, Darjeeling,  
Siliguri -734013, India

Email: rajat\_biswas@nbu.ac.in

### Abstract

Dye sensitized solar cells (DSSC) were fabricated using Rose Bengal dye. Pure and pre-dye treated Zinc oxide (ZnO) nanoparticles were used to fabricate the photoanodes of two cells. The structural characteristics of ZnO nanoparticles were studied using X-ray diffraction analysis and the surface morphology by Scanning electron microscopy. The absorption property of the dye was studied using UV-VIS spectra. The pre-dye treatment has improved the properties of ZnO, such as reduced agglomeration, improved morphology, increased dye adsorption and reduced dye aggregation. Photovoltaic parameters like short circuit current density ( $J_{sc}$ ), open circuit voltage ( $V_{oc}$ ), fill factor (FF) and overall energy conversion efficiencies ( $\eta$ ) for the conventional and pre-dye treated ZnO based fabricated cells were calculated to be  $3.73 \text{ mA/cm}^2$ ,  $0.53 \text{ V}$ ,  $0.63$  and  $1.26 \%$  and  $4.47 \text{ mA/cm}^2$ ,  $0.55 \text{ V}$ ,  $0.62$  and respectively. The pre-dye treated DSSC showed an improvement in short circuit current density ( $J_{sc}$ ) by  $19.84\%$  and efficiency ( $\eta$ ) by  $21.43 \%$ .

**Keywords:** *Dye sensitized solar cell, Alternate photoanode, ZnO Nanoparticle, Rose Bengal dye, Pre-dye treated ZnO.*

## 1. Introduction

Ever growing global energy requirement and depleting level of fossil fuels have accelerated the demand for efficient power generation from solar photovoltaic (PV) cells in recent years [1-3]. The environmental impact of the use of fossil fuels is another major concern [4]. The current production of Photovoltaic (PV) modules is dominated by crystalline silicon modules based on bulk wafers. However, the use of toxic materials and the high production cost of these solar cells have motivated the researchers to find new kinds of less expensive and non silicon-based solar cells to harvest solar energy efficiently [5-8].

Dye-sensitized solar cells (DSSCs) are a non-conventional photovoltaic technology that has attracted significant attention because of their high conversion efficiencies and low cost. O'Regan. B. & Grätzel reported high efficiency cells using nanoporous titanium dioxide ( $\text{TiO}_2$ ) semiconductor electrodes, ruthenium (Ru) metal complex dyes, and iodine electrolyte solutions in the journal of Nature in 1991 [9]. Since then, many studies have been actively carried out on DSSCs and revealed their performance comparable to amorphous silicon thin films [10, 11]. These DSSCs have the advantages of low cost, lightweight and easy fabrication, but issues include durability and further improvement of their properties. To respond to these issues, many attempts have been made, such as solidifying electrolytes and improving materials and structures, but there have been no great breakthroughs yet [12, 13].

A dye-sensitized solar cell consists of two conducting glass electrodes in a sandwich arrangement. Each layer has a specific role in the cell. The transparent glass electrodes allow the light to pass through the cell. The titanium dioxide serves as a holding place for the dye and participates in electron transfer. The dye molecules collect light and produce excited electrons which cause a current in the cell. The iodide electrolyte layer acts as a source for electron replacement. The bottom conductive layer is coated with platinum so that light does not pass through the bottom layer. A schematic structure of a liquid electrolyte DSSC and its working principle is shown in Fig. 1. When light passes through the conductive glass electrode, the dye molecules absorb the photons and the electrons in the dye go from a

ground state (HOMO) to an empty excited state (LUMO). This is referred to as photoexcitation. The excited electrons jump to the conduction band of the semiconducting dioxide and diffuse across this layer reaching the conductive electrode. Then they travel through the outer circuit and reach the counter electrode. The dye molecules become oxidized after losing an electron to the semiconductor oxide material. The red-ox iodide electrolyte donates electrons to the oxidized dye molecules thereby regenerating them. When the originally lost electron reaches the counter electrode, it gives the electron back to the electrolyte [9, 14].

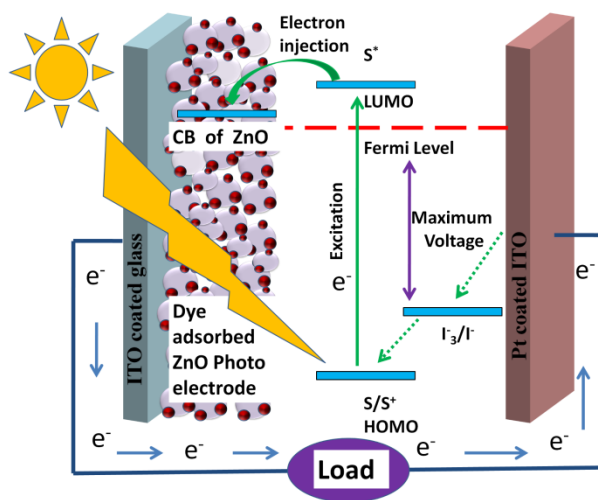


**Figure 1.** Schematic diagram and working principle of a DSSC.

The photovoltaic performance of a DSSC highly depends on all of its components and the fabrication methodology. Therefore, the optimization of every component is extremely crucial to achieve the best performance. Since its introduction into the science community in 1991, the nanocrystalline photoanode in dye-sensitized solar cells have predominantly been comprised of titanium ( $\text{TiO}_2$ ) nanoparticles as the semiconducting material [9, 14, 15]. Many researchers became very interested in studying the dye-sensitized solar cell performance fabricated using alternative semiconducting nanomaterials [16,17]. Specifically, Zinc Oxide ( $\text{ZnO}$ ) has been an ideal alternative to  $\text{TiO}_2$  because of having a similar conduction band edge that is appropriate for proper electron injection from the excited dyes; moreover,  $\text{ZnO}$

provides better electron transport due to its higher electronic mobility. Moreover, ZnO is also highly transparent, which allows greater light penetration [18-22]

In this study, ZnO nanoparticles were used to fabricate the photoanode of the DSSCs and Rose Bengal dye was utilized as a sensitizer. To obtain better efficiency, the dye molecules must bind tightly to the mesoporous ZnO photoanode surface with the assistance of their anchoring group so as to ensure proficient electron injection from the LUMO of dye molecule to the conduction band (CB) of ZnO. Here, we have studied the effect of the inclusion of rose bengal dye solution during the ZnO nanoparticle paste preparation. This yielded a coloured pre-dye treated paste of ZnO nanoparticles. The performance of pre-dye treated DSSC was compared with the cell prepared without pre-dye treating.

## 2. Materials and Method

### 2.1. Materials

Transparent ITO coated glass ( $10 \Omega/\text{square}$ ) was purchased from Techinstro, India. Commercial ZnO nanopowder, Rose Bengal dye, and Triton X-100 were bought from Sigma Aldrich, India. The liquid electrolyte used in our experiment was a Solaronix high performance electrolyte (Iodolyte AN50) with iodide/tri-iodide as redox couple, ionic liquid, and lithium salt and pyridine derivative as additives dissolved in acetonitrile solvent. The liquid platinum paint (Platisol T) purchased from Solaronix, Switzerland was used to prepare the platinum-coated transparent counter electrode. Meltonix 1170-25 ( $25\mu\text{m}$ ) purchased from Solaronix was used as a spacer between the working and counter electrode to avoid short-circuiting. All the reagents utilized in the fabrication process were of analytical grades. So no further purification was required.

### 2.2. Preparation of pure ZnO photoanode

To prepare the thin films of the photoanode materials, the ITO coated glass substrates were first cleaned with dilute HCl in an ultrasonic bath for 15 minutes and then thoroughly rinsed

with deionized water to remove the HCL residues. Then the substrates were cleaned with acetone and ethanol using an ultrasonic cleaning bath [17, 22].

The working electrode of the DSSC was prepared by following the standard doctor blade method. The paste for doctor blading was prepared by mixing ZnO nanopowder with dilute acetylacetone as a solvent and ethyl cellulose as a binder. One drop of Triton X-100 was added to the mixture to reduce the surface tension of the slurry and to enable even spreading. The mixture was stirred continuously in order to obtain smooth lump-free slurry. The ZnO paste was then coated on the conductive side of the cleaned ITO glass substrate and subsequently annealed at 450°C on a hot plate for 30 min in order to burn out the ethyl cellulose contents of the working electrode and strengthens the bonding between the substrate and the ZnO film. In addition to that, the annealing procedure also helps to improve the surface quality of the thin film along with increasing the crystallinity of the sample.

### *2.3. Preparation of pre-dye treated ZnO photoanode*

To prepare the pre-dye treated ZnO photoanode, the above procedure is slightly modified by directly adding 0.3 mM ethanolic solution of Rose Bengal dye during the ZnO nanoparticle paste preparation. This yielded a coloured pre-dye treated paste of ZnO nanoparticles. This paste was also coated on a previously cleaned ITO glass substrate and annealed following the identical procedure as followed for the pure ZnO electrode to obtain the pre-dye treated ZnO working electrode.

### *2.4. Fabrication of the cells*

Both of the pure and pre-dye treated ZnO electrodes were sensitized by immersing them in a 0.3 mM ethanolic solution of Rose Bengal dye for 12 hours. The working electrodes were then removed from the solution and thoroughly rinsed with deionized water and ethanol to get rid of any excess dye from the ZnO nanoparticle film surface and left for air drying at room temperature. The platinum catalyst precursor solution Platisol-T (Solaronix) was spin-coated on the conducting side of the cleaned ITO glasses and heated at 450 °C for 15 minutes on a hot plate to prepare the counter electrodes for the cells. The dye adsorbed working

electrodes and platinum (Pt)-coated counter electrodes were assembled against the coated sides of each other in a sandwich manner using two binder clips with a Surlyn film (Meltonix 1170-25 $\mu\text{m}$ , Solaronix) gasket as a spacer in between them. The liquid electrolyte used in the fabrication process was poured inside the cell through fine holes pre-drilled on the counter electrodes. The redox concentration of the electrolyte was 50 mM. The active area of the cells for illumination was 0.16 cm<sup>2</sup>.

### 2.5. Characterization and Measurements

PAN-analytical X'Pert PRO X-ray diffractometer (CuK $\alpha$  radiation, 30 mA, 40 kV,  $\lambda=1.5406$  Å) was used to study the crystalline structure of the ZnO nanoparticles. The surface morphology of the prepared ZnO thin films was studied by using scanning electron microscopy (JEOL). The Current-Voltage (I-V) characterization of the cells was done using a Keithley 2400 digital source meter under 100 mW/cm<sup>2</sup> illumination (Xenon lamp 450W).

## 3. Results and Discussion

### 3.1. UV-VIS absorption spectral analysis of the dye

UV-VIS absorption spectrum of the Rose Bengal dye is shown in Fig. 3. The Rose Bengal dye absorbs a larger fraction of the solar spectrum in the visible region of 460–600 nm and it shows the highest optical absorption at 549 nm wavelength.

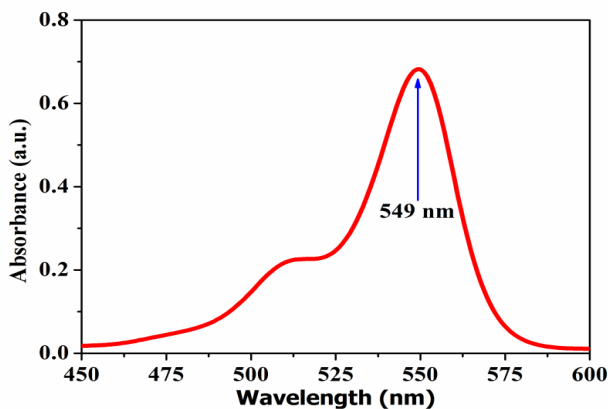


**Figure 2.** Absorption spectra of Rose Bengal dye.

### 3.2. Structural and phase characterization ZnO of the photoanode

X-ray diffraction pattern of the as-purchased ZnO nanopowder is shown in Fig. 2. The XRD pattern exhibits the hexagonal wurtzite crystal phase of ZnO and peaks well matches with the standard JCPDS card no. 36-1451. The diffraction peaks observed at  $2\theta$  values of  $31.79^\circ$ ,  $34.42^\circ$ ,  $36.25^\circ$ ,  $47.51^\circ$ ,  $56.60^\circ$ ,  $62.86^\circ$ ,  $67.96^\circ$ , and  $69^\circ$  corresponds to the reflection from the (100), (002), (101), (110), (103), (112), and (201) lattice planes respectively. Sharp and strong peaks indicate the highly crystalline nature of the material [23, 24].

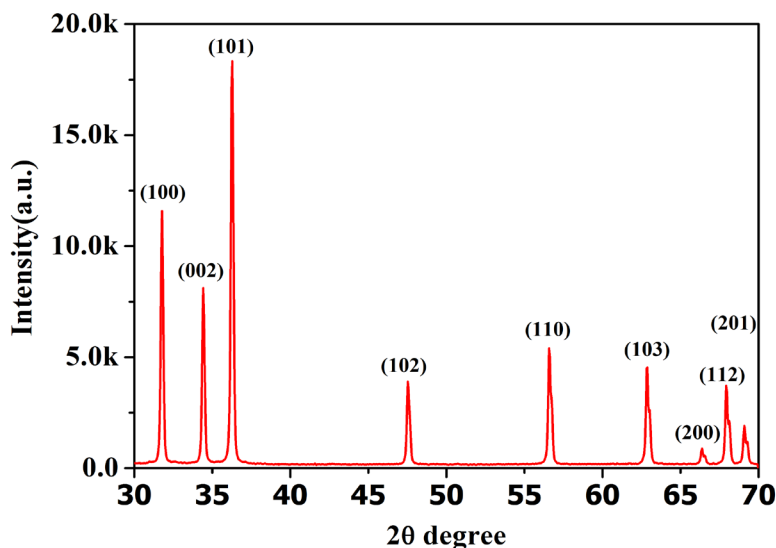


**Figure 3.** X-ray diffraction pattern of ZnO nanoparticles.

### 3.3. Surface Morphology study and energy dispersive spectroscopy of the photoanodes

Scanning electron microscopic (SEM) analysis of the ZnO nanopowder film on the ITO substrate was carried out to study the morphological properties and the particle size of the sample. The SEM image of the ZnO nanoparticles on an ITO substrate is shown in Fig.4 (a).

The SEM observation confirms that the ZnO particle size is in the nanometre range and they have hexagonal wurtzite structure. Further, the chemical composition and elemental percentage of the film are revealed by the EDS analysis which is shown in Fig. (b) and (c) respectively.

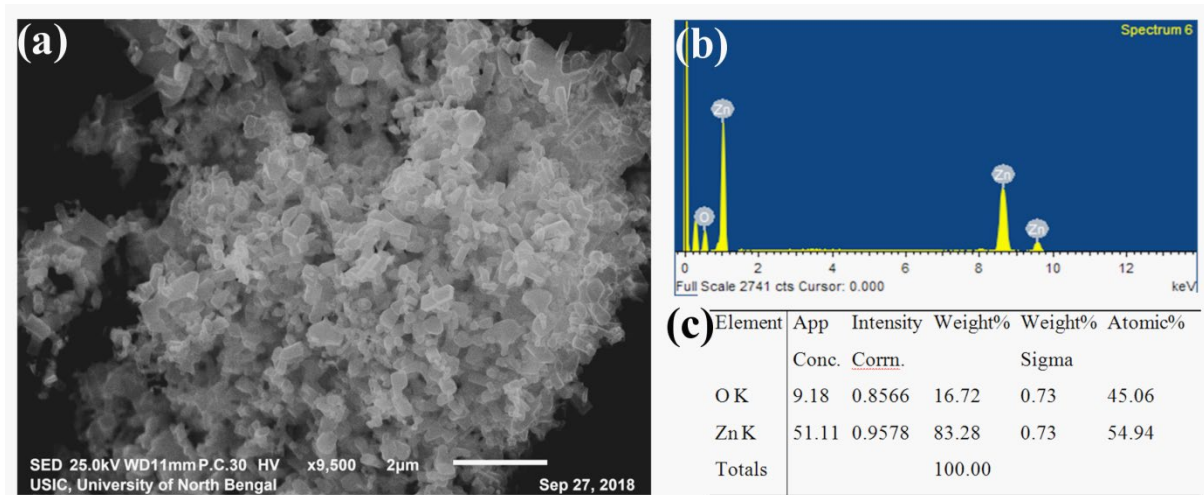


**Figure 4.** (a) SEM images, (b) EDS and (c) Elemental composition of ZnO Nanoparticles respectively

#### 3.4. Photovoltaic (Current-Voltage) characterization of the cells

The Current-Voltage characteristic is an essential measurement that reveals the values of the overall photovoltaic performance of a solar cell along with key performance parameters like open circuit voltage and short circuit current density. Fig. 5(a) depicts the I-V characteristics of the DSSCs based on pure and pre-dye treated ZnO as photoanodes respectively. The overall photoconversion efficiency of the solar cell is calculated by the formula

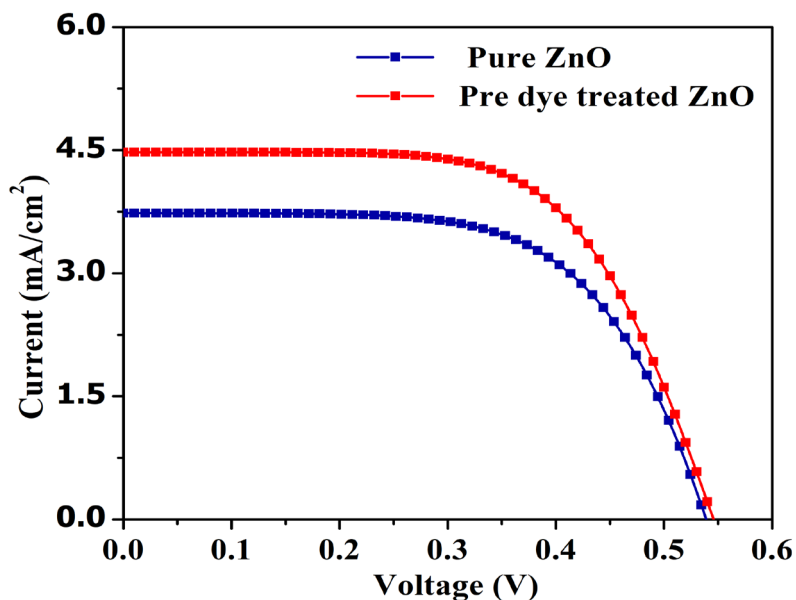
$$= \frac{P_{out}}{P_{in}} = \frac{I_{sc} V_{oc} FF}{P_{in}} \quad (1)$$

Where  $P_{in}$ ,  $V_{oc}$ ,  $I_{sc}$  and  $FF$  denote the incident photon power, open-circuit voltage, the short circuit current density and fill factor respectively. The fill factor is calculated using the following formula:



$$FF = \frac{I_{\max}V_{\max}}{I_{sc}V_{oc}} \quad (2)$$

Where  $I_{\max}$  and  $V_{\max}$ , respectively, represent values of the current and voltage at the maximum output power point of the solar cell.



The photovoltaic parameters extracted from the I-V characteristics of the fabricated DSSCs are shown in table 1 below.

**Table 1.**

Photovoltaic performance of uncoated and ZnO coated  $WO_3$  photoanode based DSSC

ZnO precursor solution concentration	$J_{sc}$ (mA/cm <sup>2</sup> )	$V_{oc}$ (V)	FF	Efficiency ( $\square$ %)
Pure ZnO	3.73	0.53	0.63	1.26
Pre-dye treated ZnO	4.47	0.55	0.62	1.53

A considerable improvement in the values of  $J_{sc}$  and  $\eta$  for the pre-dye treated DSSC can be observed compared to the conventionally prepared pure ZnO electrode from Table 1. This

demonstrates the positive role of the pre-dye treating process. This may be attributed to the fact that the pre-dye loading method resulted in uniform dye adsorption, reduced agglomeration, the improved surface morphology of photoanode and less dye aggregation [25]. The  $V_{oc}$  is also improved slightly. The increased amount of dye molecule adsorption on the pre-dye treated ZnO nanoparticle surface absorbs more photons and thereby injecting more number of electrons to the conduction band of ZnO. This yielded increased  $J_{sc}$  and  $\eta$ .

---

#### 4. Conclusion

DSSCs using pure and pre-dye treated ZnO nanoparticles as photoanode material were fabricated and their electro-optical performances were compared. The performance of the DSSC was remarkably improved upon pre-dye loading. The pre-dye treated ZnO DSSC showed a 19.84% improvement in Short circuit current density ( $J_{sc}$ ) and 21.43 % improvement in photoconversion efficiency ( $\eta$ ). Therefore, the method of pre-dye loading of ZnO nanoparticles may be used as an effective and novel way to improve the performance of dye sensitized solar cells.

#### Acknowledgment

Authors gratefully acknowledge the Dept. Of Physics, the University of North Bengal for providing financial support and laboratory facilities for carrying out the research work. JS acknowledges DST, Govt. of India for providing DST-Inspire fellowship for carrying out research work.

#### References

1. Bach W. Global warming: the complete briefing (2nd ed). John Houghton. Cambridge University Press: Cambridge, 1997. Pp. xv + 251. Paperback: ISBN 0521-62932-2, ú12.95; hardback: ISBN 0-321-62089-9, ú35.00. International Journal of Climatology. 1998;18(5):579-80.
2. Meadows DH, Meadows DL, Randers J, Behrens WW. The limits to growth. New York. 1972;102:27.

3. Minger TJ, editor Greenhouse glasnost: the crisis of global warming: essays. Greenhouse/Glasnost: the Sundance Symposium on Global Climate Change,(USA), 1989; 1990: Ecco Press.
4. Barbir F, Veziroğlu TN, Plass Jr HJ. Environmental damage due to fossil fuels use. International journal of hydrogen energy. 1990 Jan 1;15(10):739-49.
5. Goetzberger A, Hebling C, Schock HW. Photovoltaic materials, history, status and outlook. Materials Science and Engineering: R: Reports. 2003 Jan 1;40(1):1-46.
6. Alharbi F, Bass JD, Salhi A, Alyamani A, Kim HC, Miller RD. Abundant non-toxic materials for thin film solar cells: Alternative to conventional materials. Renewable Energy. 2011 Oct 1;36(10):2753-8.
7. Lee TD, Ebong AU. A review of thin film solar cell technologies and challenges. Renewable and Sustainable Energy Reviews. 2017 Apr 1;70:1286-97.
8. Yamamoto K, Yoshimi M, Tawada Y, Okamoto Y, Nakajima A. Cost effective and high-performance thin film Si solar cell towards the 21st century. Solar energy materials and solar cells. 2001 Feb 1;66(1-4):117-25.
9. B. O'regan and M. Grätzel, A low-cost, high-efficiency solar cell based on dye-sensitized colloidal TiO<sub>2</sub> films, *nature* 353, 737, (1991).
10. Chiba Y, Islam A, Komiya R, Koide N, Han L. Conversion efficiency of 10.8% by a dye-sensitized solar cell using a Ti O<sub>2</sub> electrode with high haze. Applied Physics Letters. 2006 May 29;88(22):223505.
11. Grätzel M. Solar energy conversion by dye-sensitized photovoltaic cells. Inorganic chemistry. 2005 Oct 3;44(20):6841-51.
12. Chung,I., Lee,B., Jiaqing, H.,Robert, P. H. C. & Kanatzidis, M. G. (2012). All-solid-state dye-sensitized solar cells with high efficiency.Nature, 485,7399,415-540.

13. Cai, N., Moon, S.J., Cevey-Ha, L., Moehl, T., Humphry-Baker, R., Wang, P., Zakeeruddin, S.M., & Grätzel, M. (2011). An organic D- $\pi$ -A dye for record efficiency solid-state sensitized hetero-junction solar cells. *Nano Lett.* 11, 11(4), 452–1456.
14. M. Grätzel, Dye-sensitized solar cells, *Journal of Photochemistry and Photobiology C: Photochemistry Reviews* 4, 145, (2003).
15. F. Shao, J. Sun, L. Gao, S. Yang and J. Luo, Growth of various TiO<sub>2</sub> nanostructures for dye-sensitized solar cells, *The Journal of Physical Chemistry C* 115, 1819, (2010).
16. Tiwana P, Docampo P, Johnston MB, Snaith HJ, Herz LM. Electron mobility and injection dynamics in mesoporous ZnO, SnO<sub>2</sub>, and TiO<sub>2</sub> films used in dye-sensitized solar cells. *ACS nano.* 2011 Jun 28;5(6):5158-66.
17. Biswas R, Chatterjee S. Effect of surface modification via sol-gel spin coating of ZnO nanoparticles on the performance of WO<sub>3</sub> photoanode based Dye Sensitized Solar Cells. *Optik.* 2019 Dec 28:164142.
18. Zhang Q, Dandeneau CS, Zhou X, Cao G. ZnO nanostructures for dye-sensitized solar cells. *Advanced Materials.* 2009 Nov 6;21(41):4087-108.
19. Guillén E, Peter LM, Anta JA. Electron transport and recombination in ZnO-based dye-sensitized solar cells. *The Journal of Physical Chemistry C.* 2011 Nov 17;115(45):22622-32.
20. Quintana M, Edvinsson T, Hagfeldt A, Boschloo G. Comparison of dye-sensitized ZnO and TiO<sub>2</sub> solar cells: studies of charge transport and carrier lifetime. *The Journal of Physical Chemistry C.* 2007 Jan 18;111(2):1035-41.
21. Vittal R, Ho KC. Zinc oxide-based dye-sensitized solar cells: A review. *Renewable and Sustainable energy reviews.* 2017 Apr 1;70: 920-35.
22. Biswas R, Roy T, Chatterjee S. Study of Electro-Optical Performance and Interfacial Charge Transfer Dynamics of Dye Sensitized Solar Cells Based on ZnO Nanostructures and Natural Dyes. *Journal of Nanoelectronics and Optoelectronics.* 2019 Jan 1;14(1):99-108.

23. Costantino U, Marmottini F, Nocchetti M, Vivani R. New Synthetic Routes to Hydrotalcite-Like Compounds– Characterisation and Properties of the Obtained Materials. *European Journal of Inorganic Chemistry*. 1998;1998(10):1439-46.
24. Oh J-M, Hwang S-H, Choy J-H. The effect of synthetic conditions on tailoring the size of hydrotalcite particles. *Solid State Ionics*. 2002;151(1-4):285-91.
25. Ananth S, Vivek P, Arumanayagam T, Murugakoothan P. Pre dye treated titanium dioxide nanoparticles synthesized by modified sol–gel method for efficient dye-sensitized solar cells. *Applied Physics A*. 2015 Jun 1;119(3):989-95.